

Proceedings of the International Conference on Oxide Materials for Electronic Engineering, May 29–June 2, 2017, Lviv

# Impedance Spectra of As-Grown and Heat Treated $\text{Na}_{0.5}\text{Bi}_{0.5}\text{TiO}_3$ Crystals

T.V. KRUZINA<sup>a</sup>, V.M. SIDAK<sup>a,\*</sup>, M.P. TRUBITSYN<sup>a</sup>, S.A. POPOV<sup>a</sup>, A.YU. TULUK<sup>a</sup>  
AND J. SUCHANICZ<sup>b</sup>

<sup>a</sup>Oles Honchar Dnipro National University, prosp. Gagarina 72, Dnipro, 49010, Ukraine

<sup>b</sup>Institute of Physics, Pedagogical University, Podchorazych 2, 30-084 Krakow, Poland

The complex impedance spectra  $Z^*(\omega)$  were studied for as-grown and annealed in air  $\text{Na}_{0.5}\text{Bi}_{0.5}\text{TiO}_3$  single crystals. Experimental data showed that annealing significantly increased impedance and led to appearance of low frequency  $Z^*$  relaxation. The detected relaxation processes were associated with charge transfer within the regions with initial and reduced after annealing concentration of oxygen vacancies.

DOI: [10.12693/APhysPolA.133.816](https://doi.org/10.12693/APhysPolA.133.816)

PACS/topics: 77.84.-s, 43.58.Bh, 72.80.Rj

## 1. Introduction

Sodium bismuth titanate  $\text{Na}_{0.5}\text{Bi}_{0.5}\text{TiO}_3$  (NBT) is one of the most promising lead-free piezoelectric materials with perovskite structure [1]. At room temperature NBT exhibits considerable remnant polarization, but relatively high coercive field and conduction hinder polarization switching. It is quite obvious that charge transfer is caused by the proper structural defects arising at moderate temperatures and illumination [2, 3]. To control the NBT properties valuable for practical applications, it is necessary to study the nature of the proper defects and to propose the methods to regulate their concentration.

Studying permittivity  $\varepsilon$  and conductivity  $\sigma$  in [4, 5] showed presence of  $\varepsilon$  relaxation maximum near 670 K and thermally activated growth of  $\sigma$  at  $T > 700$  K. Besides that, it was demonstrated that electrical properties strongly varied after annealing and were dependent on temperature and atmosphere of thermal treating. It turned out that after annealing in air at 870 K the relaxation peak of  $\varepsilon$  practically disappeared, whereas annealing at 1070 K significantly decreased  $\sigma$ . It was concluded that dipolar defects contributing to  $\varepsilon$  relaxation and mobile charge carriers giving rise to  $\sigma$  were formed by oxygen vacancies  $V_O$ . In this paper we study spectra of complex impedance  $Z^*(\omega)$  for as-grown and heat treated NBT single crystals.

## 2. Experimental

NBT single crystals were grown from the melts by the Czochralski method. In accordance with the procedure used in [5], concentration of  $V_O$  in the samples was controlled by heat treatment carried out in air. At the beginning spectra of  $Z^*(\omega)$  were measured for

the as-grown samples. After that the samples were annealed at  $T_1 = 870$  K for 1 h. Then the samples were cooled to room temperature and  $Z^*(\omega)$  spectra were measured on heating run. Next annealing was performed at  $T_2 = 1070$  K for 1 h after that the samples were cooled to room temperature and  $Z^*(\omega)$  spectra were measured again. Before each annealing the electrodes were removed and deposited again after heat treatment. The samples for measurements of  $Z^*(\omega)$  spectra were prepared as the plates of  $5 \times 5 \times 0.5$  mm<sup>3</sup> dimensions with (111) main planes. Platinum electrodes were deposited by magnetron sputtering in argon atmosphere at 370 K.  $Z^*(\omega)$  spectra were measured using the impedance meter Tesla BM-507 in the frequency range 5 Hz–500 kHz. The upper limits of the temperature intervals were chosen well below the corresponding annealing points. The temperature of the samples was changed in a stepwise regime and was stabilized within  $\pm 1$  K during  $Z^*$  measuring for chosen frequencies  $\omega$ . The average heating rate was about 50 K/h.

## 3. Experimental results and discussion

Figure 1 shows the impedance spectra  $Z^*(\omega)$  plotted in ( $Z''-Z'$ ) complex plane for the as-grown sample. The diagrams are presented for the temperature interval, where charge transfer processes become detectable ( $T > 700$  K), up to the temperature which was chosen well below  $T_1$ . One can see that the experimental hodographs consist of single semicircle arcs. It is known that a single arc can be described by impedance of a parallel RC circuit [6, 7]:

$$Z_1^*(\omega) = Z(\omega = 0) [1 + i\omega\tau]^{-1}, \quad (1)$$

where  $\omega$  represents cyclic frequency of measuring field,  $\tau = RC$  is impedance relaxation time. The centers of the arcs in Fig. 1 are slightly shifted down from abscissa axis  $Z'$  that is typical for real structures and can be explained by  $\tau$  distribution in the sample volume. Phenomenologically shift of the arcs centers can be described by substituting in (1) ordinary capacitance  $C$  with frequency

\*corresponding author; e-mail: [vsidak@3g.ua](mailto:vsidak@3g.ua)

dependent generalized one [6]:

$$C^* = A(i\omega)^{n-1} \quad (0 \leq n \leq 1). \quad (2)$$

Figure 2 shows the impedance spectra  $Z^*(\omega)$  of the sample annealed at  $T_1$  which demonstrate presence of two arcs. Such diagrams can be simulated by impedance of two serially connected parallel RC\* circuits

$$Z_2^*(\omega) = \left[ (R_1^{-1} + i\omega C_1^*)^{-1} + (R_2^{-1} + i\omega C_2^*)^{-1} \right]. \quad (3)$$

The experimental hodographs of the sample heat treated at  $T_2$  represent nearly ideal arcs shown in Fig. 3 and described by using (1), (2). The diagrams, calculated with the help of (1-3), are plotted in Figs. 1-3 by solid lines.

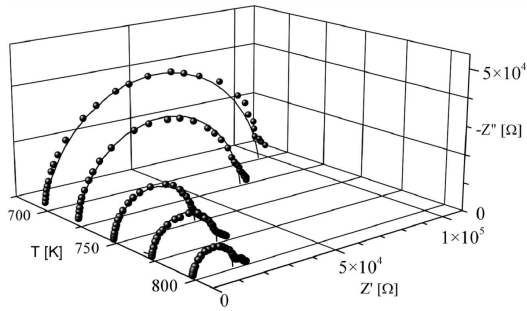


Fig. 1. Hodographs ( $Z'$ - $Z''$ ) for the as-grown NBT sample. Symbols represent the experimental data, solid lines are calculated by using the models described in the text.

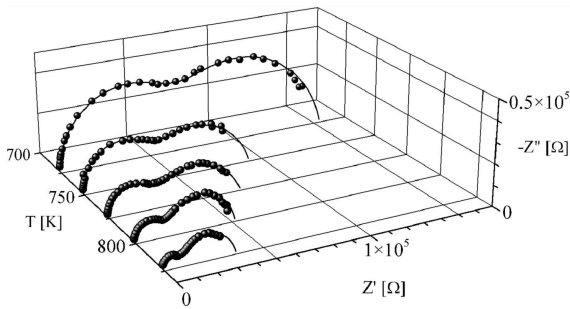


Fig. 2. Hodographs for the NBT sample annealed at  $T_1$ .

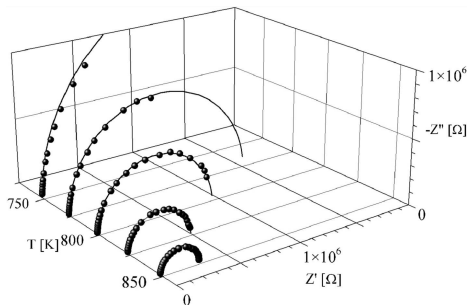


Fig. 3. Hodographs for the NBT sample annealed at  $T_2$ .

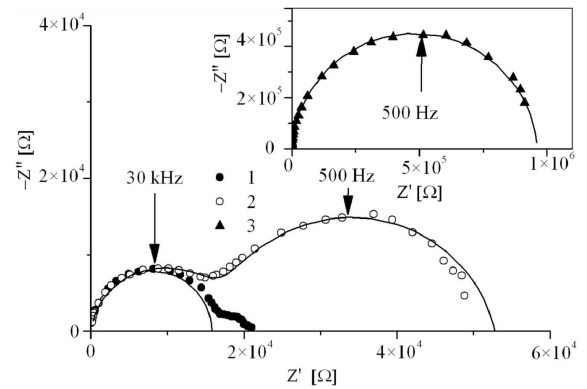


Fig. 4. Hodographs measured at  $T = 798$  K for the NBT samples: 1 — as-grown, 2 — annealed at  $T_1$ , 3 — annealed at  $T_2$ . Because of the difference in the scales, the diagram 3 is presented separately in the inset. In the hodograph for the as-grown sample (1) appearance of the low-frequency arc can be distinguished.

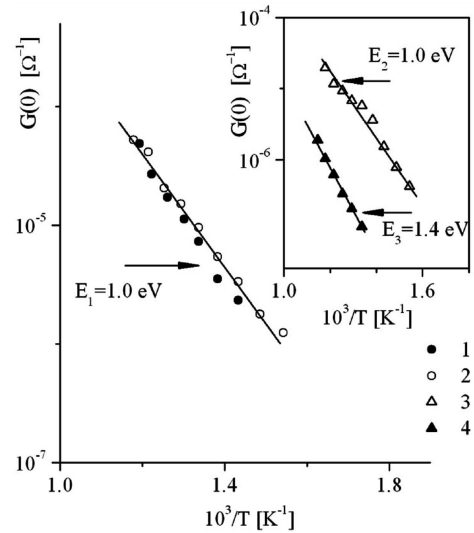


Fig. 5. Conductance at zero frequency  $G(\omega = 0)$  vs.  $1/T$  determined from the high frequency arcs in the hodographs for the as-grown sample (1), and the sample annealed at  $T_1$  (2). Inset shows dependence of  $G(\omega = 0)$  vs.  $1/T$  determined from the low frequency arcs in the hodographs for the samples annealed at  $T_1$  (3) and at  $T_2$  (4).

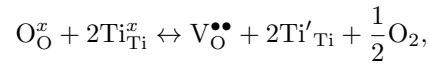
Figure 4 compares the hodographs of the studied samples. One can see that the single arc for the as-grown sample and the high frequency arc for the sample annealed at  $T_1$ , have nearly the same characteristics ( $R$ ,  $\tau^{-1}$ ) (Fig. 4). At that the spectra for the sample annealed at  $T_1$  are characterized by appearance of the additional arc, whose characteristic frequency is lower by two orders of magnitude in comparison with the high frequency arc. In the hodograph of the samples annealed at  $T_2$  only the low frequency arc can be distinguished (inset to Fig. 4). Comparison of the hodographs of the samples annealed

at  $T_1$  and  $T_2$  evidences that for the low frequency arc relaxation rate  $\tau^{-1}$  remains practically unchanged whereas arc diameter  $R = Z'(\omega = 0)$  increases more than in one order after annealing at  $T_2$ .

Obviously, that annealing in air at appropriate temperatures provides an exchange of oxygen between a sample and surrounding atmosphere that decreases  $V_O$  concentration in the structure. As it was shown in [5], annealing at  $T_1$  destroyed associated dipolar complexes but practically did not change concentration of mobile charge carriers contributing to conductivity. Thus, at not too high temperatures ( $T_1$ ) decrease of  $V_O$  content after annealing could be expected only in the near surface layer. Thus, the high frequency arcs detected for the as-grown and annealed at  $T_1$  samples (Fig. 4) can be attributed to charge transfer within the sample bulk where concentration of the mobile defects corresponds to non heat treated medium. The low frequency arcs, becoming well detectable for the sample treated at  $T_1$  and reflecting main relaxation process in the sample treated at  $T_2$ , can be associated with conduction in the regions depleted of  $V_O$  after annealing.

Using the experimental data and the expressions (1)–(3) one can calculate conductance  $G(\omega = 0) = R^{-1}$  in DC field, corresponding to the arcs observed in the hodographs (Figs. 1–3). The obtained data are plotted in Fig. 5. One can see that DC conductance corresponding to the high frequency arcs practically does not depend on annealing. Significant decrease of conductance after heat treating occurs just due to appearance of the low frequency arc which is associated with impedance of the regions depleted of  $V_O$ . Hence, main contribution to conduction can be attributed to mobile oxygen vacancies and the defects related to  $V_O$ .

The results of  $Z^*(\omega)$  spectra studying agree with the data given in [4, 5] where increase of conductivity above 700 K was connected with mobile defects associated with  $V_O$ . In the process of crystal growth oxygen vacancies arise, and electroneutrality can be ensured by electrons localized on neighboring cations. After annealing in air, oxygen vacancies are filled due to exchange with surrounding atmosphere. The quasi-chemical reaction of this process in the Kröger–Winke notation can be written as follows:



where  $O_O^x$ ,  $Ti_{Ti}^x$  represent filled neutral lattice sites,  $V_O^{\bullet\bullet}$  is oxygen vacancy,  $Ti'_{Ti}$  is titanium ion capturing an extra electron [8]. In an external electric field oxygen vacancies and captured electrons can jump over the sites, contributing to ionic and electronic charge transfer. Annealing in air reduces concentration of  $V_O$  that decreases ionic and electronic components of total conduction.

#### 4. Conclusions

Study of complex impedance spectra in as-grown and annealed NBT single crystals makes it possible to distinguish charge transfer processes in the regions depleted of oxygen vacancies after heat treating. It is shown that conduction in NBT crystals is determined by oxygen vacancies and associated with  $V_O$  defects.

#### References

- [1] T. Takenaka, H. Nagata, in: *Lead-Free Piezoelectrics*, Eds. S. Priya, S. Nahm, Springer, New York 2012, p. 255.
- [2] I.P. Pronin, P.P. Syrnikov, V.A. Isupov, V.M. Egorov, N.V. Zaitseva, *Ferroelectrics* **25**, 395 (1980).
- [3] H. Nagata, *J. Ceram. Soc. Jpn.* **116**, 271 (2008).
- [4] T.V. Kruzina, V.M. Sidak, M.P. Trubitsyn, S.A. Popov, J. Suchanicz, *Ferroelectrics* **462**, 140 (2014).
- [5] V.M. Sidak, M.P. Trubitsyn, in: *2015 International Young Scientists Forum on Applied Physics (YSF), Dnipropetrovsk (Ukraine)*, 2015.
- [6] E. Barsoukov, J.R. Macdonald, *Impedance Spectroscopy. Theory, Experiment, and Applications*, 2nd ed., Wiley, Hoboken 2005.
- [7] V.F. Lvovich, *Impedance Spectroscopy. Application to Electrochemical and Dielectric Phenomena*, Wiley, Hoboken 2012.
- [8] M. Li, H. Zhang, S.N. Cook, L. Li, J.A. Kilner, I.M. Reaney, D.C. Sinclair, *Chem. Mater.* **27**, 629 (2015).